Lateral Feedback from Monophasic Horizontal Cells to Cones in Carp Retina

II. A Quantitative Model

M. KAMERMANS, B. W. VAN DIJK, and H. SPEKREIJSE

From the University of Amsterdam, Laboratory of Medical Physics and The Netherlands Ophthalmic Research Institute, Department of Visual System Analysis, 1105 AZ Amsterdam, The Netherlands

ABSTRACT About half of the monophasic horizontal cells in carp retina receive input from both red- and green-sensitive cones. Since the horizontal cells feed back to cones, the color and feedback pathways result in wavelength- and intensity-dependent changes of the dynamics and of the receptive field amplitude profile of the horizontal cell responses. In this paper we present a quantitative model that describes adequately the color and spatial coding and the dynamics of the responses from monophasic horizontal cells in carp. Lateral feedback plays a distinct role in this model.

INTRODUCTION

About half of the monophasic horizontal cells (MHC) in carp retina receive input from both red-sensitive cones (R-cone) and green-sensitive cones (G-cone) (Yang et al., 1982, 1983; Tauchi et al., 1984; van Dijk, 1985). The synaptic input from the cones decreases the synaptic membrane resistance of the MHC and depolarizes the cell (Trifonov, 1968; Werblin, 1975). Furthermore, MHCs are electrically coupled by gap-junctions (Kaneko, 1971), which results in larger receptive fields than expected from the dendritic fields.

The receptive field amplitude profile, the sensitivity, and the dynamics of the responses from MHCs are described in an experimental paper (Kamermans et al., 1989). In that paper we propose a model in which presynaptic lateral feedback from MHCs to cones plays a prominent role. In the present paper we describe the effects of feedback on the spatial properties of the MHC network, on the dynamics of the MHC response, and on "mutual color enhancement" (Byzov et al., 1977). We will show that feedback results in a nonlinear I–V relation of the horizontal cell membrane in the network. The model describes successfully the dynamics, color, and spatial coding of the MHCs, as well as many hitherto incompletely understood findings.

Address reprint requests to Dr. H. Spekreijse, University of Amsterdam, Laboratory of Medical Physics and The Netherlands Ophthalmic Research Institute, Department of Visual System Analysis, Meibergdreef 15, 1105 AZ Amsterdam, The Netherlands.

J. GEN. PHYSIOL. © The Rockefeller University Press · 0022-1295/89/04/0695/20 $2.00
Volume 93 April 1989 695–714

THE LATERAL FEEDBACK MODEL

The proposed model, presented in Fig. 1, is based on the following assumptions: (1) The dynamics and sensitivity of the R-cones and the G-cones are the same (Spekreijse et al., 1972; van Dijk, 1985). (2) The response, I', of an isolated cone to a stimulus I, can be described by a first-order low-pass RC-filter with a time constant of 100 ms (Kaneko and Tachibana, 1985). (3) The synapse from the cone to the MHC behaves as a first-order low-pass RC-filter with a time constant of 16 ms. Schnapf and Copenhagen (1982) reported a time constant of ~16 ms for the cone/HC synapse in turtle, which fits well with data of Spekreijse and Norton (1970). (4) The MHCs are packed in a hexagonal array; i.e., each cell has six neighboring MHCs (Kaneko, 1971; Wagner, 1976; Kaneko and Stuart, 1980). All the cones above a MHC are reduced to one central cone above the MHC. (5) R- and G-cones modulate separate groups of ion channels in the MHC membrane (Trifonov et al., 1974; Byzov et al., 1977; Byzov and Trifonov, 1981); but both cone inputs modulate the same type of ion current (Na^+ current). The membrane resistance can thus be divided into four resistances: (*a*) the nonsynaptic membrane resistance, R_m, which is the resistance between the inside of the MHC and the surrounding medium, which is grounded; (*b*) the R-cone–driven synaptic membrane resistance, R_r, which is the resistance between the inside of the MHC and the surrounding medium; (*c*) the G-cone–driven synaptic membrane resistance, R_g; (*d*) the gap-junction resistance, R_c, which is the resistance between the insides of neighboring MHCs. The capacitances C_m and C_c are assumed to be parallel with the passive membrane resistance and the gap-junction resistance. (6) R_m and R_c are resistances without voltage dependency. This assumption is in contrast to that made by Byzov and his colleagues (Trifonov et al., 1974; Byzov et al., 1977; Byzov and Trifonov, 1981), and also by Werblin (1975) and Usui et al. (1983). (7) In the dark, R_r is smaller the R_g, since the R-cone system dominates the MHC response (Spekreijse and Norton, 1970; van Dijk, 1985). (8) Presynaptic feedback, I'_{fb}, from MHCs to the cones is present and I'_{fb}

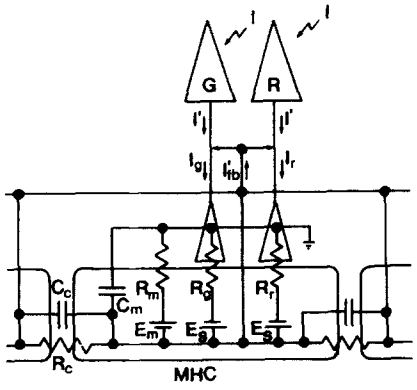

FIGURE 1. A schematic presentation of the proposed model. The following abbreviations have been used in this figure: *MHC*, horizontal cell; *R*, R-cone; *G*, G-cone; R_r, R-cone–modulated synaptic membrane resistance; R_g, G-cone–modulated synaptic membrane resistance; R_m, nonsynaptic membrane resistance; R_c, coupling resistance; E_s, equilibrium potential of the ion channels of the nonsynaptic membrane resistance; E_m, equilibrium potential of the G-cone–modulated synaptic membrane resistance; C_c, capacity of the gap-junction; C_m, capacity of the horizontal cell nonsynaptic membrane; I, light input; I', response of isolated cone; I'_{fb}, feedback signal from the horizontal cell pool; I_r, horizontal cell input from the R-cone system; I_g, horizontal cell input from the G-cone system.

changes linearly with the membrane potential of the MHC. (9) Each cone receives a feedback signal from a pool of surrounding MHCs. This pool reflects the extensive receptive field overlap of horizontal cells in carp. We have assumed that feedback extends up to a third neighbor, and that the contribution by the neighboring cells decreases with distance. In the model we have chosen, rather arbitrarily for the following weighing factors: central cell, 1.0; first ring of neighboring cells, 1.0; second ring, 0.75; third ring, 0.5. (10) The feedback synapse from the MHC to the cone is a first-order low-pass RC-filter with a time constant of 100 ms. This value fits the data of the experimental paper best (Kamermans et al., 1989). (11) A pure delay of 25 ms exists in the feedback pathway. This is based on the common finding that the red component of the response of the biphasic horizontal cell (BHC), which is believed to be the signal from the MHC that is fed back to the cones (Stell and Lightfoot, 1975), has a delay of 25 ms (Spekreijse and Norton, 1970).

The MHC Model Network

If hexagonal stimuli, which are aligned with the network, are used then the two-dimensional hexagonal resistor network (Fig. 2 *a*) can be transformed by a one-dimensional network (Fig. 2 *b*) (Usui et al., 1983). One of the reviewers pointed out that the transformation from the two-dimensional to the one-dimensional network of Usui does not hold for radially symmetric stimuli. Since radially symmetric stimuli are used in the experiments described in the accompanying paper (Kamermans et al., 1989) an error will result. This error is most prominent for cells in the periphery. Their potential will be underestimated and therefore R_c will be overestimated. Also, the lateral feedback strength will be overestimated but no qualitative differences are to be expected. Since, however, the model parameters are relative, the values of R_c and the lateral feedback strength should not be considered as estimates of the parameters in the retina. Because the MHCs are strongly coupled, no large difference in amplitude between neighboring MHCs is to be expected. For the above reasons we believe that the spots may be approximated by hexagons.

All calculations are performed in the equivalent one-dimensional network that consists of 10 cells.

According to the laws of Kirchoff, the following equation must hold in point $V[1]$ (Fig. 2 *b*):

$$i_1 + i_2 + i_3 + i_4 + i_5 = 0 \tag{1}$$

with:

$$i_1 = (V[1] - E_m)/R_m \tag{2}$$

$$i_2 = C_m\, dV[1]/dt \tag{3}$$

$$i_3 = (V[1] - E_s)/R_s[1] \tag{4}$$

$$i_4 = 6(V[1] - V[2])/R_c \tag{5}$$

$$i_5 = 6C_c\, d(V[1] - V[2])/dt \tag{6}$$

$$R_s[n] = \frac{R_r[n]R_g[n]}{R_r[n] + R_g[n]} \tag{7}$$

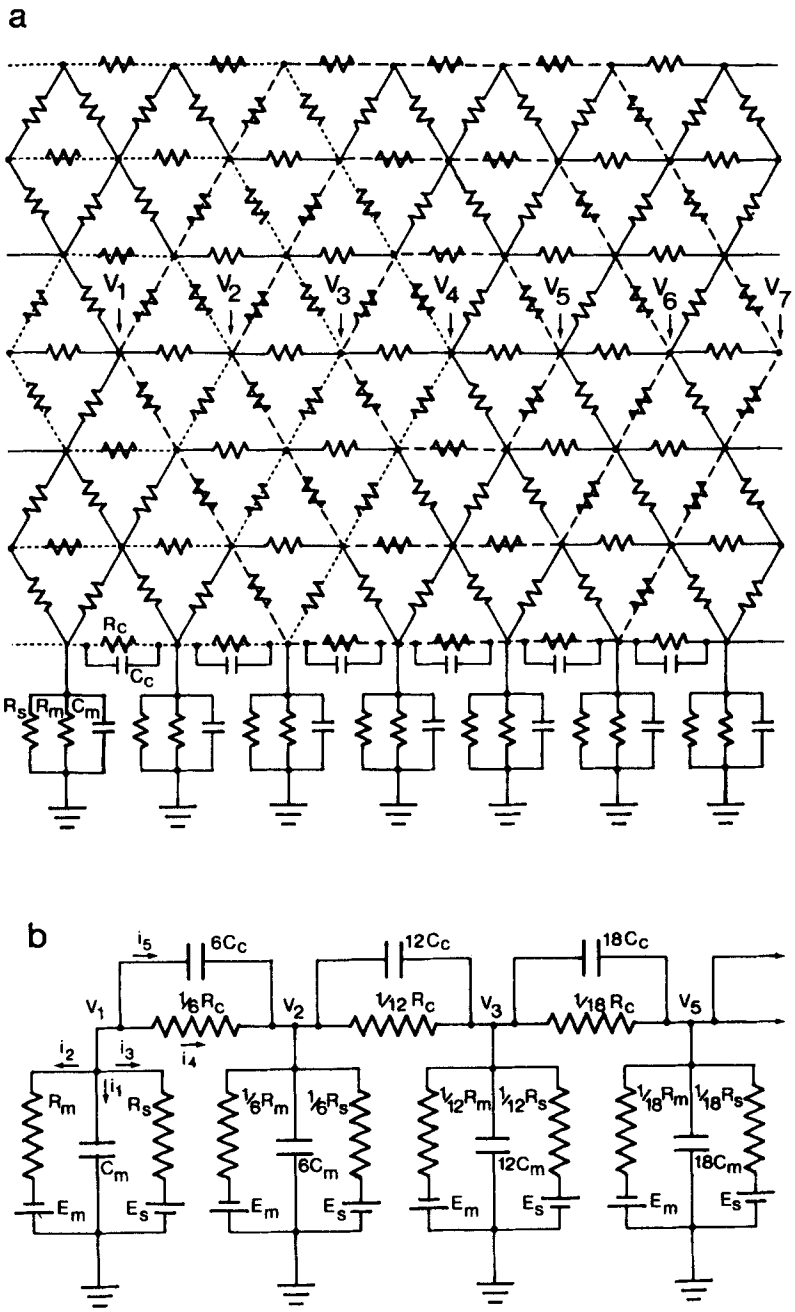

FIGURE 2. (*a*) A schematic two-dimensional description of the lateral feedback model. The dotted lines represent points with equal potential when a spot stimulus is used; $V[2]$, $V[3]$, and $V[4]$, respectively. The dashed lines represent cells with equal feedback to cell number 4. (*b*) A schematic one-dimensional description of the lateral feedback model for the spot stimuli. For the meaning of the symbols see text.

where: $V[n]$, potential difference between the inside of the model cell and ground; E_s, equilibrium potential of the ion channels of the synaptic membrane resistance; E_m, equilibrium potential of the ion channels of the nonsynaptic membrane resistance; C_m, membrane capacitance; C_c, gap-junction capacitance; $R_r[n]$, R-cone–modulated synaptic membrane resistance of the nth cell; $R_g[n]$, G-cone–modulated synaptic membrane resistance of the nth cell; R_c, resistance of the gap-junction; R_m, resistance of the nonsynaptic membrane resistance. From these equations we can solve $V[1]$, or in the same way, $V[n]$. This gives the following expressions for spot stimuli. For $n = 1$:

$$V[1] = \frac{R_m R_c R_s[1]}{R_m R_c + R_c R_s[1] + 6R_m R_s[1]} \left\{ \frac{E_s}{R_s[1]} + \frac{E_m}{R_m} + 6\frac{V[2]}{R_c} - C_m \frac{dV[1]}{dt} - 6C_c \left[\frac{d(V[1] - V[2])}{dt} \right] \right\} \tag{8}$$

For $1 < n < 11$:

$$V[n] = \frac{R_m R_c R_s[n]}{R_m R_c + R_c R_s[n] + [(2n-1)/(n-1)] R_m R_s[n]} \left\{ \frac{E_s}{R_s[n]} + \frac{E_m}{R_m} + \frac{n}{n-1}\frac{V[n+1]}{R_c} + \frac{V[n-1]}{R_c} - C_m \frac{dV[n]}{dt} - C_c \left[\frac{n}{n-1} \frac{d(V[n] - V[n+1])}{dt} + \frac{d(V[n] - V[n-1])}{dt} \right] \right\} \tag{9}$$

The formulas for slit stimuli in the one-dimensional network are found in the same manner. Because cell number 1 is the center of symmetry of the network for the slit stimuli, it has two first neighbors. Thus:

$$i_1 + i_2 + i_3 + 2i_4 + 2i_5 = 0 \tag{10}$$

$V[1]$ and $V[n]$ can now be solved. For $n = 1$:

$$V[1] = \frac{R_m R_c R_s[1]}{R_m R_c + R_c R_s[1] + 2R_m R_s[1]} \left\{ \frac{E_s}{R_s[1]} + \frac{E_m}{R_m} + 2\frac{V[2]}{R_c} - C_m \frac{dV[1]}{dt} - 2C_c \left[\frac{d(V[1] - V[2])}{dt} \right] \right\} \tag{11}$$

For $1 < n < 11$:

$$V[n] = \frac{R_m R_c R_s[n]}{R_m R_c + R_c R_s[n] + 2R_m R_s[n]} \left\{ \frac{E_s}{R_s[1]} + \frac{E_m}{R_m} + \frac{V[n+1]}{R_c} + \frac{V[n-1]}{R_c} - C_m \frac{dV[n]}{dt} - C_c \left[\frac{d(V[n] - V[n+1])}{dt} + \frac{d(V[n] - V[n-1])}{dt} \right] \right\} \tag{12}$$

For both networks $V[11]$ is the potential of $V[1]$ in the dark.

Input

With $I(n)$ the stimulus, the response of the isolated cones above the nth cell, $I'[n]$, can be described by a first-order low-pass RC-filter with a time constant of 100 ms (Eq. 13). From this signal the feedback signal from the MHC, $I'_{fb}[n]$, is subtracted after multiplication with the feedback constants (*fbr* and *fbg*), which reflect the efficiency and number of the feedback synapses. This combined signal is filtered by the synaptic filter, a first-order low-pass RC-filter with a time constant of 16 ms. The final output of the cone, $I_r[n]$ or $I_g[n]$, is the input for the MHC (Eq. 14, a and b).

$$I'[n] = I[n] - 0.1\, dI'[n]/dt \tag{13}$$

$$I_r[n] = (I'[n] - fbr \cdot I'_{fb}\,[n]) - 0.016\, dI_r[n]/dt \tag{14a}$$

$$I_g[n] = (I'[n] - fbg \cdot I'_{fb}\,[n]) - 0.016\, dI_g[n]/dt \tag{14b}$$

The ratio of the input to the R- and G-cones varies with stimulus wavelength as given by the spectral characteristics of the R- and the G-cone system (Spekreijse et al., 1972; van Dijk and Spekreijse, 1984). For 500- and 520-nm stimuli the ratio of the inputs to the R- and the G-cone system is 1:4. Only the R-cone system is assumed to receive input for the 670- and 694-nm stimuli.

Synaptic Membrane Resistance

The synaptic membrane resistances, $R_r[n]$ and $R_g[n]$, are modulated by the input from the cones. They each consist of two resistances in series: a constant resistance (R_r° or R_g°) and a variable resistance. R_r° is the resistance that remains in the R-cone–modulated channels when all R-cone–modulated channels are open. R_{rs} and R_{gs} are the values of the synaptic membrane resistances when feedback is inactive. The equations for $R_r[n]$ and $R_g[n]$ are:

$$\begin{aligned} &\text{if } R_r[n] \le R_r^\circ, \quad \text{then } R_r[n] = R_r^\circ \\ &\text{if } R_r[n] > R_r^\circ, \quad \text{then } R_r[n] = R_{rs} + k \cdot I_r[n] \end{aligned} \tag{15a}$$

$$\begin{aligned} &\text{if } R_g[n] \le R_g^\circ, \quad \text{then } R_g[n] = R_g^\circ \\ &\text{if } R_g[n] > R_g^\circ, \quad \text{then } R_g[n] = R_{gs} + k \cdot I_g[n] \end{aligned} \tag{15b}$$

where k is a constant that describes the relation between the presynaptic current and the changes in postsynaptic membrane resistance.

Lateral Feedback

The lateral feedback signal is the summed feedback signal of each cell and of its three neighboring cells in any direction (Eq. 10). Since the stimulus is always centered above cell number 1, a rather complex relation describes the feedback via the cones to the nth cell for spot stimuli. Fig. 2 *a* shows $V[2]$, $V[3]$, and $V[4]$ as dotted lines in the two-dimensional network. The dashed lines around cell number 4 indicate cells with equal feedback to cell number 4. We find the Eq. 16 a–c by counting the feedback to the first, second, and third cell. Eq. 17 is the generalized feedback

equation for $n \geq 4$.

$$I_{fb}[1] = V[1] + 6 \cdot V[2] + 9 \cdot V[3] + 9 \cdot V[4] \quad (16a)$$

$$I_{fb}[2] = V[1] + 7.75 \cdot V[2] + 6 \cdot V[3] + 6.75 \cdot V[4] + 3.5 \cdot V[5] \quad (16b)$$

$$I_{fb}[3] = 0.75 \cdot V[1] + 4 \cdot V[2] + 5.5 \cdot V[3] + 6.5 \cdot V[4] + 5.5 \cdot V[5] + 4 \cdot V[6] \quad (16c)$$

$$\begin{aligned} I_{fb}[n] = {} & 0.5 \cdot V[n-3] + 1.75 \cdot V[n-2] + 3.5 \cdot V[n-1] \\ & + 5.5 \cdot V[n] + 5.5 \cdot V[n+1] + 4.75 \cdot V[n+2] + 3.5 \cdot V[n+3] \end{aligned} \quad (17)$$

Feedback for slit stimuli is symmetric around the nth cell; with cell $(-n)$ = cell $(+n)$ one finds:

$$\begin{aligned} I_{fb}[n] = {} & 2 \cdot V[n-3] + 3.25 \cdot V[n-2] + 4.5 \cdot V[n-1] \\ & + 5.5 \cdot V[n] + 4.5 \cdot V[n+1] + 3.25 \cdot V[n+2] + 2 \cdot V[n+3] \end{aligned} \quad (18)$$

The feedback signal is filtered by a first-order low-pass RC-filter, the feedback synapse, with a time constant of 100 ms (Eq. 19), and then multiplied with the feedback constants (*fbr* and *fbg*) (Eq. 14 a and b).

$$I'_{fb}[n] = I_{fb}[n] - 0.1\, dI'_{fb}\,[n]/dt \quad (19)$$

Parameter Values

The behavior of the model will be described under different stimulus conditions using a set of parameters that yields similar response behavior in the 10-cell network as found in reality. The following values for the various parameters were used:

$R_r^\circ = 5.5$ kΩ $\quad R_m = 10.0$ kΩ $\quad C_c = 2\ \mu$F $\quad k = 1$ kΩ/μA

$R_{rs} = 15.0$ kΩ $\quad R_c = 1.5$ kΩ $\quad C_m = 0.1\ \mu$F

$R_g^\circ = 19.0$ kΩ $\quad E_s = +10$ mV $\quad fbr = 0.19$

$R_{gs} = 30.0$ kΩ $\quad E_m = -80$ mV $\quad fbg = 0.15$

Note that these values are only valid for the 10-cell network and that only the ratios of the resistances and the time constants are relevant for the model behavior.

MODEL BEHAVIOR

In the model, feedback is present in the dark, and thus the cones will receive a hyperpolarizing input from the MHC in the dark. In the dark the membrane potential in the model settles at −19 mV; the feedforward and the feedback signal are balanced. R_r and R_g are above threshold and become $R_r = 6.0$ kΩ and $R_g = 22.9$ kΩ. The finding that the system floats in the dark has major implications for the behavior of the model as will be shown below.

Responses to Full Field Stimuli

Fig. 3 gives the model responses to 670- and 520-nm full field flashes of 500 ms. The four pairs of panels show responses at various stimulus intensities. The top

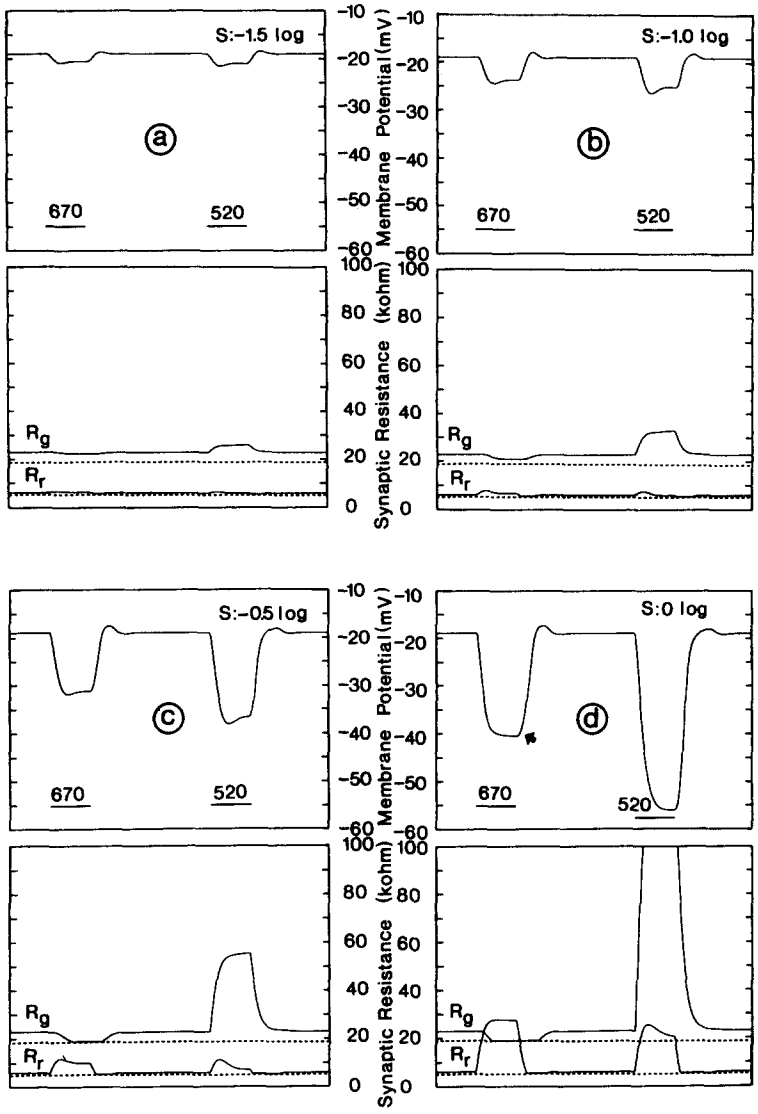

FIGURE 3. Responses of the model to 520- and 670-nm full field stimuli of 500 ms. Top of each pair, membrane potential; bottom of each pair, R_g and R_r, respectively. The timing of the stimulus is indicated with bars. (*a*) Stimulus intensity, −1.5 log. (*b*) Stimulus intensity, −1.0 log. (*c*) Stimulus intensity, −0.5 log. (*d*) Stimulus intensity, 0.0 log. R_r° and R_g° are marked with dotted lines.

panel in each pair shows the membrane potential, $V[1]$, and the bottom panel the synaptic membrane resistances, R_r and R_g. The stimulus cycle is indicated at the bottom of each panel. Stimulus intensities are indicated in each figure. Note that R_r and R_g are above their thresholds, R_r° and R_g°, which are represented by dotted lines. When a 670-nm flash is presented, the R-cone input, and thus R_r, increases. For low

intensities (Fig. 3, *a–c*) R_r remains lower than R_g and the changes in R_r determined the response waveform for the most part. Therefore, the response waveforms and amplitudes for 670- and 520-nm low intensity test flashes are more or less equal. For high stimulus intensities, however, (Fig. 3 *d*) R_r becomes larger than R_g. As a result, the response is shunted by R_g and further changes in R_r will have little influence on the response waveform. In other words, the response to 670-nm full field flashes will saturate at a level that is determined by a complete opening of all G-cone–modulated channels (i.e., R_g°).

For responses to 520-nm full field test flashes both R_r and R_g are modulated and the shunting effect of R_g, as described for 670-nm stimuli, is absent. So, the maximal response amplitude at 520 nm can become much larger than a 670-nm test flash.

It can also be understood why the repolarizing phase is not correlated with response amplitude for full field flashes. The repolarizing phase is due to feedback from the MHC to the cones. For intense 670-nm stimuli repolarization will not occur because R_g is at threshold and thus cannot be changed further by feedback. The repolarization will therefore be limited. For a response with the same amplitude evoked by a 520-nm full field flash, feedback produces a much stronger repolarization because both R_r and R_g are modulated by the feedback (Fig. 3 *c*). Note that the repolarizing phase of the MHC response cannot be explained by assuming a voltage-dependent change in the nonsynaptic membrane resistance, since this would be wavelength independent and repolarization would then be correlated with response amplitude.

The width of the response at half maximum response amplitude does not correlate with response amplitude. The response of the model to a 670-nm, 0-log full field test flash has an amplitude of 21 mV (measured just before the off response) and a width of 590 ms. The responses to a 520-nm, 0-log or −0.5-log full field test flashes have amplitudes of 38 and 18 mV, and widths of 540 and 510 ms, respectively. This broadening of the response to long wavelength stimuli is due to the slow change of R_g to values above threshold, which causes the membrane potential to depolarize very slowly at the start of the off response (Fig. 3, arrow). When R_r becomes roughly equal to R_g, the depolarization will speed up because the shunting R_g is absent.

Model Responses to Slit Stimuli

In the experimental paper (Kamermans et al., 1989) we showed that for high intensities the receptive field amplitude profile is steeper for 520-nm stimuli than for 670-nm stimuli.

Fig. 4 gives the response amplitude for the slit centered above cell number 1 as a function of cell number. In the center R_r and R_g are increased by the cone input and decreased by the feedback. In the periphery the membrane potential is hyperpolarized due to the electrotonic spread in the MHC network, and depolarized due to feedback. The reduction in R_r and R_g due to feedback will be greater the larger the amplitude of the response of the central cell. In other words, feedback will result in a steepening of the receptive field amplitude profile, and this steepening will be most pronounced when the stimulated cells respond most vigorously, i.e., when the 520-nm stimulus is used.

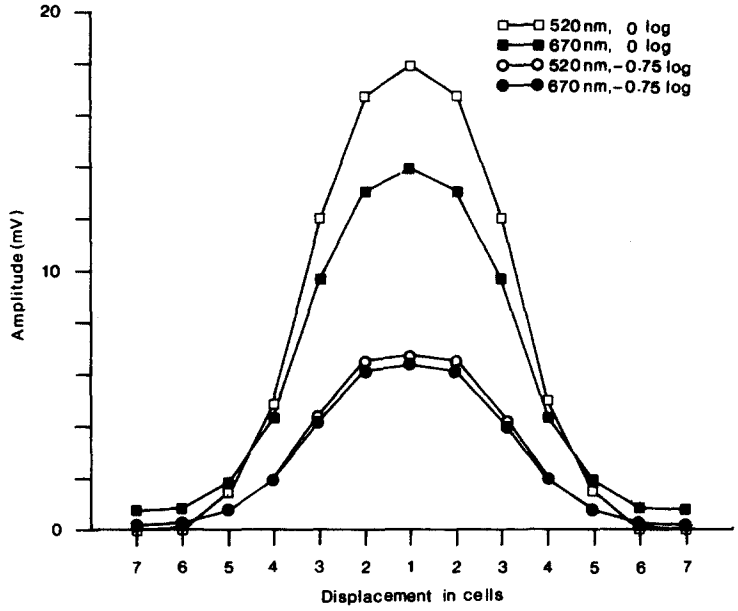

FIGURE 4. Simulation of receptive field response amplitude profiles. The square indicate the receptive field response amplitude profile for a stimulus intensity of 0 log (filled symbols, 670 nm; open symbols, 520 nm). The circles indicate the receptive field response amplitude profiles for −0.75 log. The cell number is plotted horizontally.

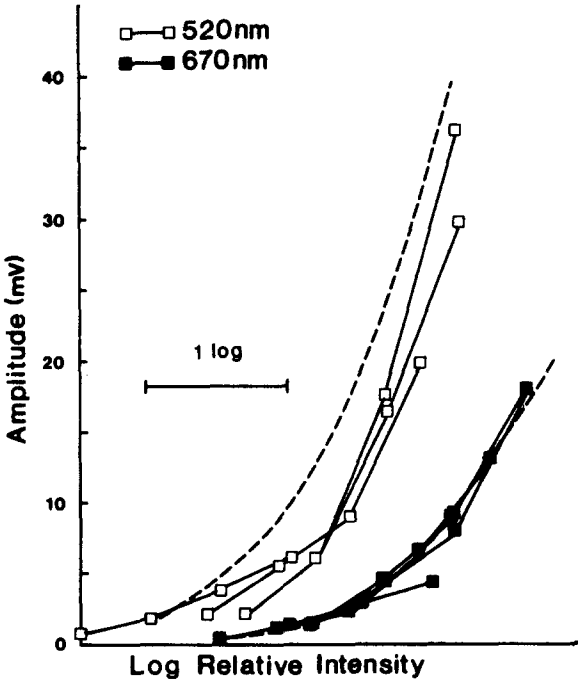

FIGURE 5. Response amplitude vs. relative log intensity curves for four spot diameters are depicted: one, three, five, and ten cells, respectively, for spots of 670- of 520-nm wavelengths (open symbols, 520 nm; filled symbols, 670 nm) The 670-nm curves were shifted along the log intensity axis until they coincided. The 520-nm curves were shifted over the same distance as the 670-nm curves, and for clarity, over 1 log unit in addition. The dashed lines show the curves when no feedback is present.

Model Responses to Spot Stimuli

Fig. 5 gives the amplitude vs. log intensity curves for various spot sizes for 670- and for 520-nm test flashes. The dashed lines are the curves in case there is no feedback. R_r and R_g are adjusted so that the dark membrane potential is equal to the dark membrane potential when feedback is present; R_r = 6.0 kΩ and R_g = 22.9 kΩ. The amplitude vs. log intensity curves become more curved when feedback is present and this change is largest for large spots. The influence from lateral feedback on the responses is most outspoken for the 520-nm flashes. Comparing Fig. 5 with Fig. 4 of the experimental paper (Kamermans et al., 1989) shows that the model can explain fully the spot size- and wavelength-dependent change of the amplitude vs. log intensity curves in MHCs.

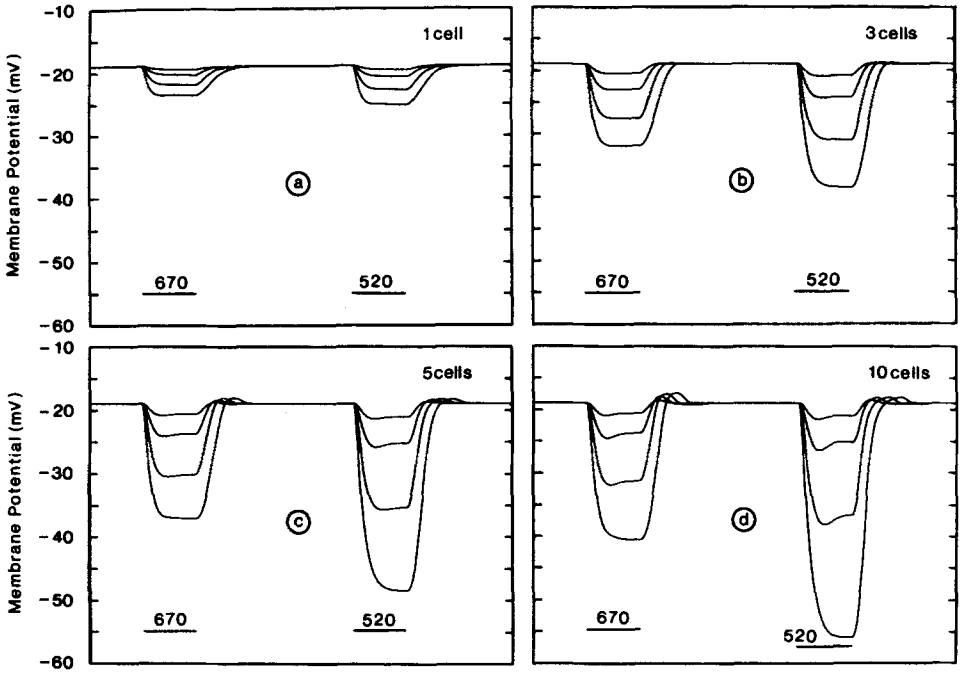

FIGURE 6. Simulated response to 520- and 670-nm test flashes of 500 ms. (*a*) Stimulus diameter, one cell. (*b*) Stimulus diameter, three cells. (*c*) Stimulus diameter, five cells. (*d*) Stimulus diameter, ten cells. Four different intensities were used: 0, −0.5, −1.0, and −1.5 log.

Fig. 6 depicts the responses to spots of four different sizes: covering one cell in Fig. 6 *a*, three cells in Fig. 6 *b*, five cells in Fig. 6 *c* and ten cells in Fig. 6 *d*, at two test wavelengths and four intensities changing in steps of 0.5 log units. The repolarizing phase from feedback is only pronounced for large spots and for 520-nm test wavelength. For small spots the feedback pool receives too little input to modify the response, while for 670-nm stimuli, R_g is at its threshold, R_g°, and shunts the response. The model behavior is highly similar to that of the MHC responses.

Effects of Chromatic Adaptation on the Model Responses

Fig. 7 gives the model responses in chromatic adaptation experiments as described in the experimental paper (Kamermans et al., 1989). Responses to 520- and 670-nm test flashes are depicted for various chromatic backgrounds. Stimulus and background wavelengths are indicated in the figure. The background intensity is increased in steps of 0.5 log units, the stimulus intensity is −0.65 log.

When a 670-nm stimulus is used on a 694-nm background (Fig. 7 *a*) the MHC is hyperpolarized by the background illumination; R_g will be lowered to its threshold (R_g°) while R_r will increase. For high background intensities the steady hyperpolarization is close to the saturation level for 670-nm test flashes. So, R_g will shunt the response and, therefore, the response amplitude to the 670-nm test flashes decreases with increasing background intensity.

When a 500-nm background is used both R_r and R_g increase. R_g increases more than R_r due to the difference in sensitivity of the G- and R-cone systems. For 670-nm flashes at low background intensities (Fig. 7 *b*) the shunting effect of R_g is reduced and an increase of the response results. For high background intensities the total synaptic membrane resistance becomes larger than R_m and synaptic input will be less effective in modulating the membrane potential.

For low intensity 694-nm backgrounds the steady hyperpolarization is mostly determined by R_r because it is lower than R_g. Modulation of R_r by the 520-nm test flash (Fig. 7 *c*) will be less effective because the total synaptic membrane resistance approaches R_r and a response reduction follows. For high background intensities, R_r is higher than R_g. The response is now mostly determined by R_g. The change of R_g by the 520-nm flash is much greater than that of R_r and so the response amplitude increases.

With a 520-nm stimulus on a 500-nm background (Fig. 7 *d*) the response amplitude is reduced over the entire intensity range. R_r and R_g are both increased by the background and the total synaptic membrane resistance becomes close to or higher than R_m. Modulation of both R_r and R_g will have little influence on the total membrane resistance and the response amplitude will decrease. Also, in this respect the model behaves like the real MHC responses.

The overshoot of the model off responses, which does not correlate with the response amplitude, is caused by a decrease of R_r towards its threshold value caused by feedback. When a low intensity chromatic background is present, R_r is more above its threshold than in the dark and the overshoot will increase (see Fig. 7). Again the behavior of the model matches the experimental data (Kamermans et al., 1989).

To demonstrate the effect of feedback on the "mutual color enhancement" we have carried out a chromatic adaptation simulation experiment with (Fig. 8, top) and without (Fig. 8, bottom) feedback. The response amplitudes just before the off response are plotted as a function of background intensity. The triangles represent the response to 670-nm test flashes and the squares depict the responses to 520-nm backgrounds. When feedback is absent, response enhancement is much smaller because the response reduction due to the increase of the total synaptic membrane resistance will be larger than with feedback.

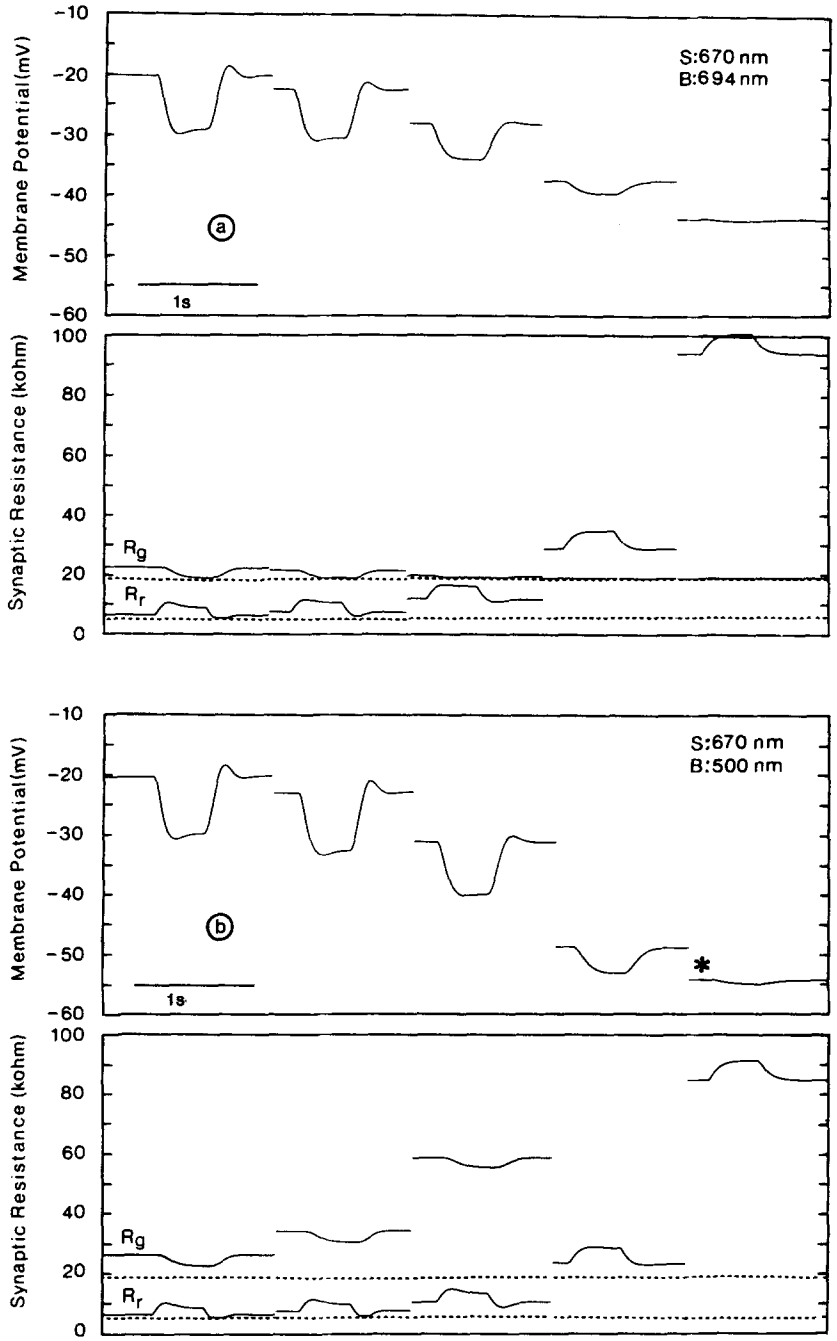

FIGURE 7. Model responses to full field flashes on backgrounds of different wavelengths and intensities. Four pairs of panels are presented. The top panel of each pair depicts the membrane potential, the bottom panel depicts R_r and R_g. Background intensity is increased in steps of 0.5 log units. The lowest background intensity, -1.5 log units, is at the left side and the highest background intensity, 0.5 log is to the right side. Stimulus and background wavelengths are indicated in the text. The traces marked with * are shifted 10 mV up. R_r° and R_g° are marked with dotted lines.

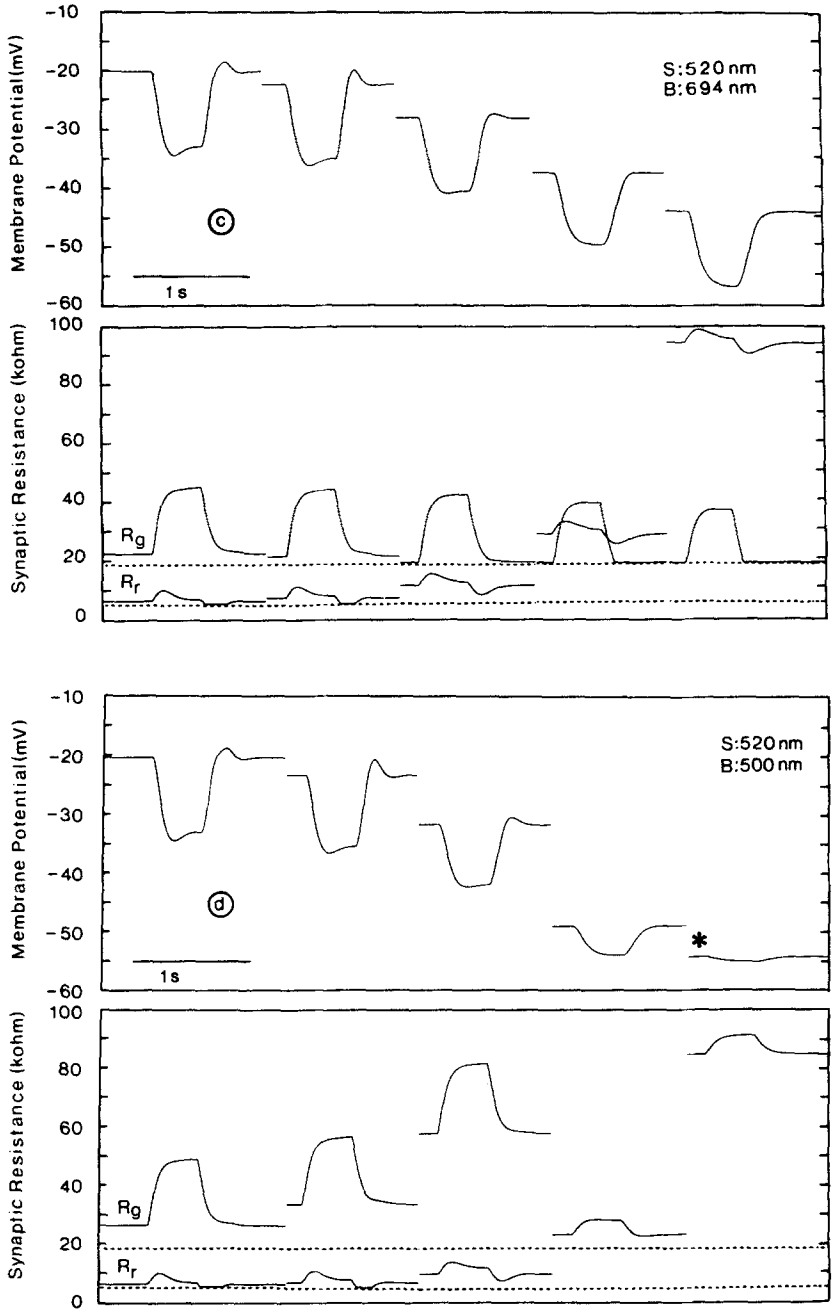

FIGURE 7 continued

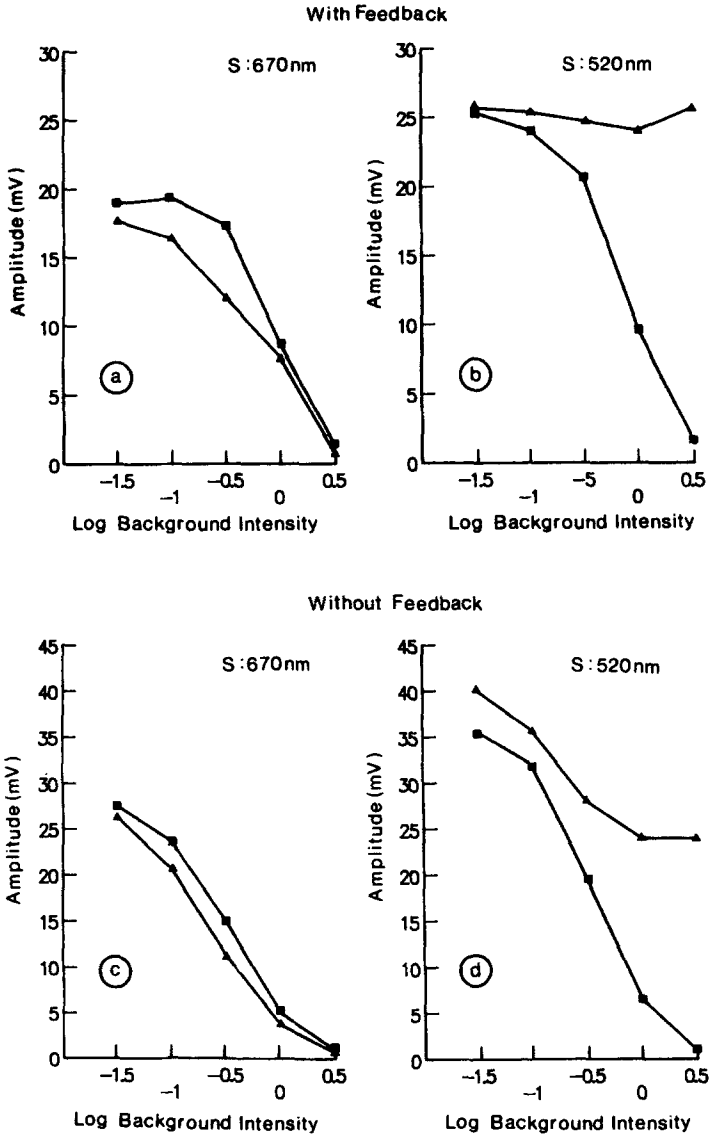

FIGURE 8. Response amplitude of the model responses are plotted against background intensity. The squares represent data for a 500-nm background wavelength and the triangles represent data for a 694-nm background wavelength. The stimulus intensity is −0.65 log. The response amplitude is measured just before the response offset. (*a*) Stimulus 670 nm with feedback. (*b*) Stimulus 520 nm with feedback. (*c*) Stimulus 670 nm without feedback. (*d*) Stimulus 520 nm without feedback.

DISCUSSION

We have chosen a single set of parameters for all simulations in this paper. Yet, we do not believe that these values are representative for the MHC network in carp retina. The values are only valid for the 10-cells network. Since the time constants change with temperature (Schellart et al., 1974), all time constants used are based on temperatures ~20°C. The spatial dimensions of the model are given in number of cells. Because of the limited number of cells, edge effects are clearly present. For most of the simulations we believe that the edge effects induce only quantitative changes. The response of the model to slit stimulus, however, shows a repolarizing phase, which is not found in MHC recordings (Fig. 1 of Kamermans et al., 1989). In the periphery even depolarizing responses can occur at high stimulus intensities. The repolarizing phase diminishes when R_c is decreased. We believe that this difference between model response and cell response is due to the limited number of cells in our model. We used slightly different parameters for R_r° and R_c for the slit simulations, since for slit stimuli the effects of the borders of the model are more pronounced. The values of the parameters were $R_r^\circ = 4.0$ kΩ and $R_c = 1.0$ kΩ.

Variations in the parameters do influence response properties only in a quantitative manner.

Lowering of R_r° results in an increase of the feedback and a stronger depolarizing overshoot. For low values of R_r°, oscillations in the responses occur, which are observed infrequently in MHC responses.

R_g° determines the maximal hyperpolarization to 670-nm test flashes. We have chosen such a value of R_g° that the difference in response amplitude for high intensity 520- and 670-nm test flashes were as in the real experiments.

When R_r and R_g were at thresholds in the dark, no overshoot or steepening of the receptive field amplitude profile occurred. Changes of the ratio R_{gs}/R_{rs} changes the spectral sensitivity of the model cell.

The capacitances C_m and C_c do not have a large influence on the response behavior. The response becomes more gradual if the capacities are increased.

E_m, E_s, and the ratio R_m/R_s determine the membrane potential in the dark. When the difference between E_s and E_m is large, modulation of R_s results in more vigorous responses. Increase of R_c reduces the receptive field diameter and makes the repolarization become more pronounced, as do the "edge effects."

The packing (Eq. 4) influences the feedback strength from the surround in the spot model. An increase of the number of neighbors will increase the strength of the feedback and will reduce the error made by the approximation of spot with hexagons. The influence of this approximation is discussed in the theoretical section.

The assumption that feedback is present over a distance of three cells in each direction must be seen in perspective of the receptive field size of the model. The receptive field size for 670-nm stimuli measured with spots of different sizes is approximately six cells. So, a feedback area that is smaller than the receptive field of the MHC can explain the phenomena described in this and the experimental paper (Kamermans et al., 1989). Dendritic overlap or telodendria are likely candidates for the lateral feedback pathway.

Changes in the feedback constants have large effects on the dynamics of the response and "mutual color enhancement" as explained above.

Changes in the time constant of the cone MHC synapse do not influence greatly the dynamics of the model response. A decrease in the time constant of the feedback synapse results in a slow oscillation in the repolarizing phase of the response. An increase in this time constant results in a slower repolarization. Shortening of the delay in the feedback pathway reduces the repolarizing phase and the depolarizing overshoot.

In summary, R_r°, R_g°, and the feedback constants are the most sensitive parameters of the model.

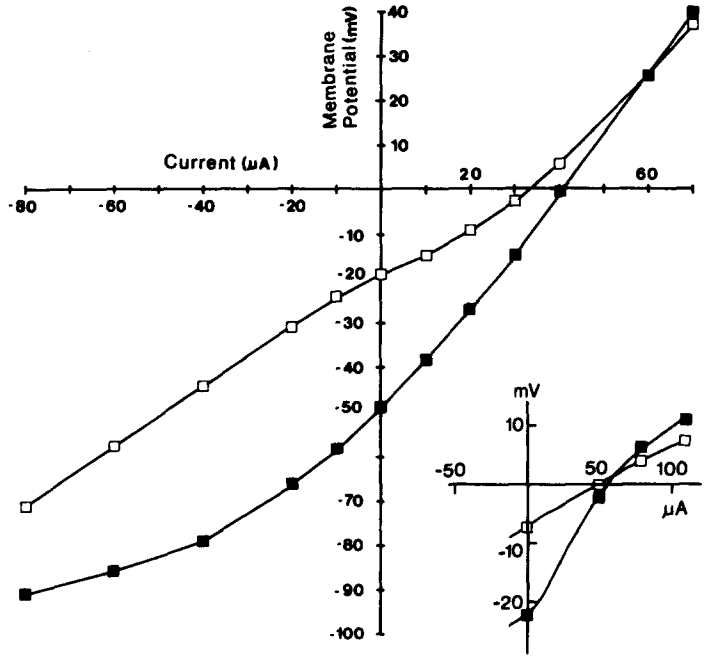

FIGURE 9. *I-V* relation of the model cells. Open symbols, no background illumination; filled symbols, 520 nm, 0 log, full field background. All cells received the same current. (*Inset*) *I-V* relation of a MHC as measured in pike retina by Trifonov et al. in the dark and with a saturating background illumination. (Redrawn after Fig. 8 *a* from Trifonov et al., 1974; with permission of Byzov.)

Comparison with Other Studies

Our model agrees with unexplained data presented in several studies on MHC responses in fish retina. Yang and colleagues (Yang et al., 1983) demonstrated an interaction between R- and G-cone input in MHCs in goldfish. Response enhancement was demonstrated to be present only when a green test flash preceded a red test flash. Yang et al. (1983) assumed that the R- and G-cone inputs were independent and that the MHC receives hyperpolarizing input from R- and G-cones and that the MHC feeds back to the G-cones. It was also assumed that stimulation with green light suppresses the feedback and enhances a subsequent response. This model cannot be true. The chromatic background experiments demonstrate that

the response enhancement depends on the intensities of the stimulus as well as on the background intensity. Furthermore, response enhancement can be found for both red and green stimuli depending on which background intensities are used.

Usui and colleagues (1983) proposed a "spatial reduction model" that consisted of eight cells to describe his results. One of the main differences between Usui's model and ours is that in his model the input resistance of the HC does not change, which is not correct as shown by, amongst others, Trifonov (1968) and Werblin (1975). Moreover, Usui postulated a potential-dependent coupling resistance. This is not necessary to explain his results. Our model shows that, due to the change of synaptic membrane resistance and the feedback, the effective coupling between the horizontal cells changes. This change is wavelength and intensity dependent.

Some indications for a feedback mechanism can be found in the work of Byzov and co-workers (Byzov et al., 1972; Trifonov et al., 1974; Byzov et al., 1977, Byzov and Cervetto, 1977) on pike and turtle retina. They reported that the nonlinear *I-V* relation found in light in pike retina becomes linear in the dark. This is in agreement with our model. In the dark, R_r and R_g are low. When the membrane potential is changed by current injection, the feedback will change and so will R_r and R_g. Fig. 9 gives the result of a simulated current injection experiment in our model of the MHC layer. All cells in the model received the injected current and the light stimuli covered all cells. The *I-V* relation is given in the dark (open symbols) and with an intense 500-nm background (filled symbols). In the dark the feedback signal can reduce R_r and R_g only to threshold. Therefore, no or only a weak nonlinear *I-V* relation will be found. The small deviation of linearity can easily be missed in current injection experiments due to the noise in the recordings. In the presence of background illumination both R_r and R_g are above threshold, and thus feedback will change them. This results in a nonlinear *I-V* relation. The similarity between our simulation data (Fig. 9) and the current injection data of Trifonov et al. (1974) (inset of Fig. 9) is striking.

Furthermore, depolarization of the HC membrane in pike retina leads to an increase of the space constant (Byzov et al., 1972). This is similar to the slit displacement experiments presented in this paper. Depolarization of the HC membrane reduces lateral feedback and so the space constant increases.

From the work of Tachibana (1981) on solitary cells, however, it can be concluded that a nonlinear membrane resistance does exist. What the main reason is for the nonlinear behavior of the MHCs in the intact retina, i.e., feedback or a nonlinear nonsynaptic membrane resistance or both, is not clear, but as discussed above our data cannot be explained with the assumption of a nonlinear *I-V* relation of the HC membrane alone, while the results from intact retina cited above can be explained in terms of our model.

We are grateful to Dr. A. L. Byzov for his valuable comments on the manuscript.

This work was supported by the Netherlands Organization for Scientific Research (NWO) through the foundation for Biophysics. B. W. van Dijk is a recipient of the Constantijn and Christiaan Huygens Fellowship from NWO.

Original version received 16 June 1988 and accepted version received 20 October 1988.

REFERENCES

Byzov, A. L., and L. Cervetto. 1977. Effect of applied currents on turtle cones in darkness and during the photoresponse. *Journal of Physiology.* 265:85–102.

Byzov, A. L., Y. A. Trifonov, and L. M. Chailahian. 1972. Effect of polarization of horizontal cells of the pike retina and spread of their electrical potentials. *Neirofiziologiya.* 4:90–96.

Byzov, A. L., Y. A. Trifonov, L. M. Chailahian, and K. W. Golubtzov. 1977. Amplification of graded potentials in horizontal cells of the retina. *Vision Research.* 17:265–273.

Byzov, A. L., and Y. A. Trifonov. 1981. Ionic mechanisms underlying the nonlinearity of horizontal cell membrane. *Vision Research.* 21:1573–1578.

Kamermans, M., B. W. van Dijk, H. Spekreijse, and R. C. V. J. Zweypfenning. 1989. Lateral feedback from monophasic horizontal cells to cones in carp retina. I. Experiments. *Journal of General Physiology.* 93:000–000.

Kaneko, A. 1971. Electrical connections between horizontal cells in the dogfish retina. *Journal of Physiology.* 213:95–105.

Kaneko, A., and A. E. Stuart. 1980. Coupling between horizontal cells in the carp retina examined by diffusion of Lucifer Yellow. *Biological Bulletin.* 159:468–480.

Kaneko, A., and M. Tachibana. 1985. Electrophysiological measurements of the spectral sensitivity of three types of cones in the carp retina. *Japanese Journal of Physiology.* 35:355–365.

Schellart, N. A. M., H. Spekreijse, and T. J. T. P. van den Berg. 1974. Influence of temperature on retinal ganglion cell response and E.R.G. of goldfish. *Journal of Physiology.* 238:251–267.

Schnapf, J. L., and D. R. Copenhagen. 1982. Differences in the kinetics of rod and cone synaptic transmission. *Nature.* 296:862–864.

Spekreijse, H. and A. L. Norton. 1970. The dynamic characteristics of color-coded S-potentials. *Journal of General Physiology.* 56:1–15.

Spekreijse, H., H. G. Wagner, and M. L. Wolbarsht. 1972. Spectral and spatial coding of ganglion cell responses in goldfish retina. *Journal of Neurophysiology.* 35:73–86.

Stell W. K. and D. O. Lightfoot. 1975. Color-specific interconnections of cones and horizontal cells in the retina of the goldfish. *Journal of Comparative Neurology.* 159:473–502.

Tauchi, M., X. L. Yang, and A. Kaneko. 1984. Depolarizing responses of L-type external horizontal cells in the goldfish retina under intense chromatic background. *Vision Research.* 24:867–870.

Tachibana, M. 1981. Membrane properties of solitary horizontal cells isolated from goldfish retina. *Journal of Physiology.* 321:141-161.

Trifonov, Y. A. 1968. Study of synaptic transmission between photoreceptors and horizontal cells by electrical stimulation of the retina. *Biofizika.* 13:809-817.

Trifonov, Y. A., A. L. Byzov, and L. M. Chailahian. 1974. Electric properties of subsynaptic and nonsynaptic membranes of horizontal cells in fish retina. *Vision Research.* 14:229–241.

Usui, S., G. Mitarai, and M. Sakakibara. 1983. Discrete nonlinear reduction model for horizontal cell response in the carp retina. *Vision Research.* 23:413–420.

van Dijk, B. W. 1985. The functional organization of carp and goldfish retina. An electrophysiological study of color interactions in vertebrate retina. PhD thesis, University of Amsterdam.

van Dijk, B. W., and H. Spekreijse. 1984. Color fundamentals deduced from carp ganglion cell responses. *Vision Research.* 24:211–220.

Wagner, H. J. 1976. The connectivity of cones and cone horizontal cells in a mosaic-type teleost retina. *Cell Tissue Research.* 175:85–100.

Werblin, F. S. 1975. Anomalous rectification in horizontal cells. *Journal of Physiology.* 244:639–657.

Yang, X. L., M. Tauchi, and A. Kaneko. 1982. Quantitative analysis of photoreceptor inputs to external horizontal cells in the goldfish retina. *Japanese Journal of Physiology.* 32:399–420.

Yang, X. L., M. Tauchi, and A. Kaneko. 1983. Convergence of signals from red-sensitive and green-sensitive cones onto 1-type external horizontal cells of the goldfish retina. *Vision Research* 23:371–380.